

Geophysical Research Letters

RESEARCH LETTER

10.1029/2020GL091041

Key Points:

- Two sharp gradients in dry spell frequency are found across southern Africa
- Trend analysis suggests that the diagonal (NW-SE) gradient has weakened during 1982–2019
- Wet days have significantly increased in several important agricultural areas in southern Africa

Supporting Information:

- Supporting Information S1

Correspondence to:

C. J. C. Reason,
Chris.Reason@uct.ac.za

Citation:

Thoithi, W., Blamey, R. C., & Reason, C. J. C. (2021). Dry spells, wet days, and their trends across southern Africa during the summer rainy season. *Geophysical Research Letters*, *48*, e2020GL091041. <https://doi.org/10.1029/2020GL091041>

Received 28 SEP 2020
 Accepted 25 JAN 2021

Dry Spells, Wet Days, and Their Trends Across Southern Africa During the Summer Rainy Season

Wanjiru Thoithi¹, Ross C. Blamey¹, and Chris J. C. Reason¹ 

¹Oceanography Department, University of Cape Town, Rondebosch, Western Cape, South Africa

Abstract Dry spell frequency and wet day occurrence during the summer rainy season across southern Africa are examined using daily rainfall for 1982–2019. Evidence shows two sharp gradients in dry spell frequency, extending southeast from southern Angola to the African south coast near the westernmost boundary of preferred cloud band occurrences (diagonal gradient), and west from the Limpopo River Valley along 22–24°S (meridional gradient) (along 14–16°S in early summer) related to regional topography. Trend analysis suggests that the diagonal gradient has weakened during 1982–2019 along with some other large areas in southern Africa whereas this is only true for part of the meridional gradient. Contrastingly, wet days and Normalized Difference Vegetation Index have significantly increased in several important agricultural areas in southern Africa. Evidence suggests these changes are related to those in the midlevel Botswana High, El Niño Southern Oscillation, Southern Annular Mode, and subtropical Indian Ocean dipole.

Plain Language Summary Rainfall across southern Africa is highly variable. Thus, the region is prone to drought and flooding events on a wide range of time scales which poses a great challenge to the large poor rural population who rely heavily on rainfed agriculture for food production. Daily rainfall data were used to examine the frequency of wet days and 5-days dry periods during the main rainy season (December-February) as well as early summer (October-November), key characteristics which tend to be more useful for farmers and water resource managers than seasonal rainfall totals. El Niño Southern Oscillation, the Southern Annular Mode, and the South Indian Ocean Dipole together with the Botswana High were found to be related to changes in dry spells and wet days. Trends in these characteristics were computed to identify significant areas of change across particularly sensitive and agriculturally important gradient regions of southern Africa.

1. Introduction

Many impoverished rural areas in southern Africa rely on rainfed agriculture with substantial intraseasonal through multidecadal rainfall variability (Reason et al., 2006; Tyson, 1986). Here, rainy season characteristics such as dry spell frequency and moderate wet day occurrences (10–30 mm/day), which are of great interest to user groups, are examined.

Dry spells and days with too intense rainfall represent opposites of the rainfall spectrum during the wet season. Too frequent an occurrence of either is unfavorable for agriculture since crops prefer consistently distributed rainfall throughout the growing season. Large anomalies in dry spell/wet day occurrences rather than seasonal totals more likely lead to widespread crop failures and hence, severe hardship for communities. Since 2014, poor and erratic rainfall, with extended dry spells throughout the summer, led to major food security concerns for much of southern Africa (FEWS NET, 2020).

Earlier studies assessed summer (December-February, DJF) dry spell frequencies over southern Africa as a whole (Usman & Reason, 2004) or for smaller subregions (Hachigonta & Reason, 2006; Reason et al., 2005) but are limited by coarse resolution (2.5°) data and relatively short periods (around 20 years). Thus, an objective is to better understand dry spells and moderate rain days (given their suitability for agriculture) over southern Africa using much higher resolution data (0.05°) for a considerably longer period (38 years). A second objective is to assess trends in these characteristics since it appears there has been no systematic study of such across southern Africa.

2. Data and Methodology

Since sufficient daily station data are unavailable, Climate Hazards Group InfraRed Precipitation with Station (CHIRPS) rainfall (0.05° grid-resolution, 1982–2019) (Funk et al., 2015) was used to compute characteristics across southern Africa for DJF as well as October–November (ON) (early crop season, important for potential malaria outbreaks, Landman et al., 2020). Following Usman and Reason (2004), a dry spell was computed as a 5-day period (pentad) with <5 mm; this criterion was found suitable for the subcontinent as a whole as well as in Limpopo (Reason et al., 2005), southwestern Tanzania (Mapande & Reason, 2005), and Zambia (Hachigonta & Reason, 2006).

The moderate wet day definition (10–30 mm/day) follows since the staple maize crop needs rainfall of ~400–600 mm during its germination/growth phases (~110 days) and because southern African rainfall is convective, any given season is unlikely to be made up of numerous light rain days (few mm/day). Maize is well adapted to rainfall coming via thunderstorms producing ~20–30 mm as long as these are spaced out through the summer. Thus, moderate wet days are more likely to contribute to the accumulated amount of rainfall needed for each crop phase (Tadross et al., 2009). The upper 30 mm threshold was selected because heavy rainfall may reduce crop yields due to water logging, soil erosion and nutrient leaching (Munodawafa, 2012; Phillips et al., 1998; Tadross et al., 2007).

To assess spatial variations, intensity-frequency maps were produced. These plot the number of seasons out of the maximum of 38 at each grid-point that contain at least half or more of the 18-pentad DJF season consisting of dry spells and the number of seasons which have at least 20 moderate wet days out of the total 90-days season respectively (and similarly for the 60 days ON season).

Maps of trends in the frequencies of dry spells and moderate wet days were evaluated using the Theil-Sen slope estimator (Sen, 1968; Theil, 1950) and the nonparametric Mann-Kendall test (Kendall, 1975; Mann, 1945). These methods are relatively insensitive to outliers with the Mann-Kendall test making no assumption about the distribution of the underlying data. Statistical significance was assessed at the 95% level.

Normalized Difference Vegetation Index-3rd generation (NDVI-3g) from GIMMS was used to consider vegetation impacts. These 1/12° resolution data are available at 15-days intervals for 1982–2015 (Pinzon & Tucker, 2014).

3. Dry Spell Frequencies

Figure 1b shows mean DJF distributions of dry spell frequency across southern Africa with several prominent features. Low frequency stands out over the Congo, Lesotho/eastern South Africa and Madagascar, all convective hotspots at this time of the year with consistent rainfall facilitated by orographic lifting of moist unstable airmasses, especially the Drakensberg and Madagascar. Very high frequency occurs in the coastal Namib desert and extends east over Namibia into the western Kalahari Desert and south into the western Karoo and Mediterranean-type climate of southwestern South Africa. As a result, two strong gradients in dry spell frequency exist during DJF in southern Africa (Figure 1a). More pronounced is the NW-SE gradient (termed diagonal gradient) across the western margins of the Kalahari Desert that runs through southern Angola, Namibia, southern Botswana, and central South Africa and which roughly marks the western boundary of the preferred continental cloud band location (Fauchereau et al., 2009; Hart et al., 2013). These cloud bands often originate from the Angola Low whose preferred position is evident in the area of low dry spell frequencies over southeastern Angola/northeastern Namibia.

The other strong gradient (termed meridional gradient) extends from central Namibia/Botswana to northern South Africa with maximum dry spell frequency centered on the Limpopo River valley (LRV). Thus, the LRV appears as a region with inconsistent rainfall distribution despite it being located close to the major moisture sources of the tropical western Indian Ocean and southwest Indian Ocean (Rapolaki et al., 2019, 2020). Again, topography plays a role since the Mozambique Channel Trough which results from the dynamical adjustment of the easterly trade winds to the Madagascan mountains acts to divert moisture away from the LRV (Barimalala et al., 2018, 2020). The lower topography of the LRV is less favorable to convective

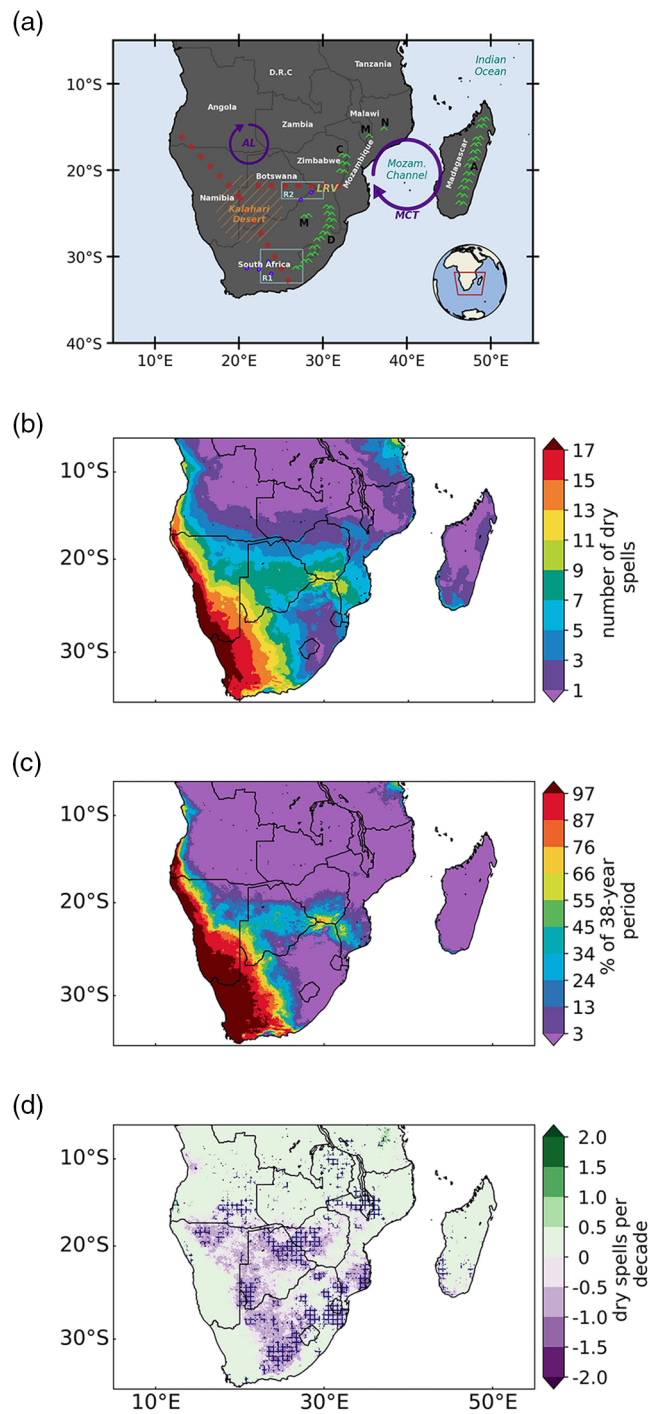


Figure 1. (a) Schematic of the key features discussed in the text. Green “^” symbols show mountain features (D = Drakensburg, C = Chimanimani, M in South Africa = Magaliesberg, M in Malawi = Mulange, N = Namuli), purple circles denote cyclonic circulation features (Mozambique Channel Trough [MCT] and Angola Low [AL]) and red dashed lines the mean location of the “diagonal” and “meridional” dry spell gradients, R1 and R2 are representative regions analyzed for the diagonal and meridional gradients. Pink dots show the location of rainfall stations used in the supplementary information. (b) DJF dry spell frequency climatology (shaded contours in pentads), (c) intensity-frequency map showing the percentage of the total number of seasons which consist of at least nine dry spells out of a maximum possible of 18, and (d) DJF dry spell frequency trends (dry spells decade⁻¹). Hatching denotes areas of significant trends calculated over the period 1981/1982–2018/2019. DJF, December-February.

development than the higher ground to its north and south. Other topographic influences leading to very low frequency can be observed on the windward side of the Chimanimani Mountains on the central Zimbabwe/Mozambique border and near Johannesburg (~26°S) due to the Magaliesberg. Outside urban areas, the latter is an important agricultural region (mainly maize). Although broadly comparable to Usman and Reason (2004), the higher resolution CHIRPS data allow a much better representation of both gradients and topographic influences (Figure 1b) as well as the identification of others (e.g., Johannesburg) which could not be seen in the 2.5° resolution data used by these authors. The early summer (ON) has not previously been considered. While the diagonal gradient remains similar, the meridional gradient is now located across the tropics (~14–16°S, Figure S1a) reflecting the imminent NE monsoon over East Africa.

Figure 1c (intensity-frequency map) shows how many of the 38 DJF seasons during 1982–2019 experienced more than half of a given summer (18 pentads) as containing dry spells indicating the vulnerability of different parts of southern Africa to dry spells. The purple areas (10% or less of the summers experiencing more than half of that season as dry) in subtropical southern Africa essentially mark the extent of the agricultural crop area (mainly maize) where rainfall is more consistent and where cloud band activity and random air mass thunderstorms are most common (Blamey et al., 2017; Hart et al., 2013).

The two gradients seen in Figure 1b are again evident with the LRV standing out in the meridional case. Here, between 75% and 90% of these DJF seasons are dry for more than half of each season. On average, the LRV appears to be as susceptible to summer dry spells as the western Kalahari Desert in southwestern Botswana/southeastern Namibia, posing great challenges for its rural population. This region surrounding the Zimbabwe/South Africa border is therefore one where the population is particularly vulnerable to multiyear droughts (Blamey et al., 2018; Malherbe et al., 2012; Reason et al., 2005). Extending west along 20–24°S (roughly the boundaries of the meridional gradient) from the LRV is a region where at least 50% of the summers contain more than half the summer rainy season as dry spells, termed the drought corridor across subtropical southern Africa by Usman and Reason (2004). For ON (Figure S1b), there is an additional E-W drought corridor across the tropics extending over the hydroelectric dams on the Zambezi River which are crucial for Zambia and Zimbabwe's electricity supply.

The coarser CMAP data used by Usman and Reason (2004) extended over the ocean and, as a result, had several inconsistencies. These included maximum dry spell intensity over coastal Mozambique/western Mozambique Channel near 22–24°S and a much less tightly defined drought corridor. The high-resolution CHIRPS data not only highlights the vulnerable LRV better but also that the highest intensity over southern Mozambique is confined to the region near the border with northeastern South Africa and does not extend all the way to the coast. Further topographic influences are also apparent; e.g., the small area of relatively high intensity south of the drought corridor in northern South Africa (~24°S) which is near the Waterberg and downstream of the northern Drakensberg. This small area is used more for cropping than less consistent rainfall regions (~22°S) which contain livestock or wildlife farms.

Given the susceptibility of the region to drought, it is interesting seeing whether the recent observational record displays any significant trend in dry spell frequency (Figure 1d). Significant decreasing trends in DJF dry spell frequency are evident over central South Africa/western Botswana/northern Namibia along the diagonal gradient and over northern Botswana/western Zimbabwe and northeastern South Africa (part of LRV meridional gradient). Figures 1c and 1d suggest that the diagonal gradient in high dry spell intensity stretching from northeastern Namibia/western Botswana to central South Africa (Figure 1b) may have weakened and shifted further west during 1982–2019. Since this region is very important for livestock farming and is on the margins of the South African maize growing area, this has important agricultural implications if it were to continue or strengthen further. Note, however, that the region also experiences considerable decadal rainfall variability (Blamey et al., 2018; Tyson, 1986). At present, the trend magnitude in the significant regions is of order 1–2 less dry spells per decade. Further north, parts of the LRV as well as southeastern Mozambique also show significant decreasing trends in dry spell frequency. Thus, in the drought corridor region, there is also a tendency for reduced dry spell frequency in some key areas suggesting a tendency toward more consistent rainfall. For ON (Figure S1c), the diagonal gradient as well as the Angola Low shows the opposite, i.e., increasing dry spells, implying decreased rainfall, consistent with CMIP5 projections over southern Africa of early summer drying (Munday & Washington, 2019).

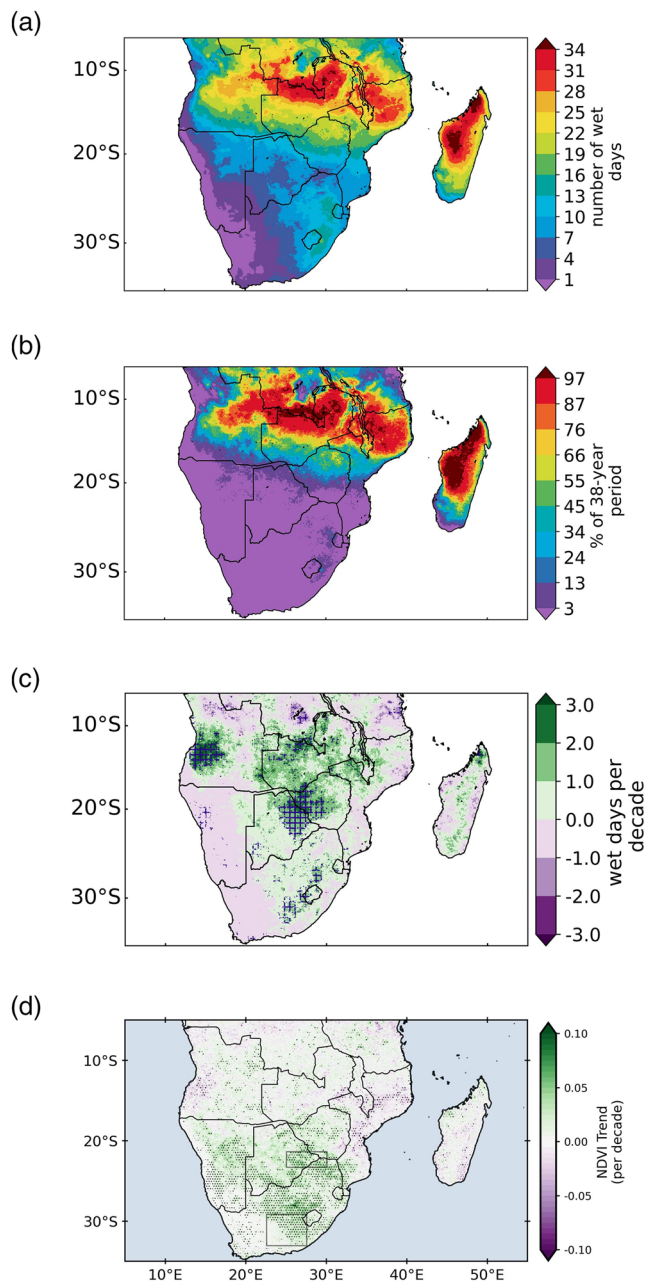


Figure 2. DJF moderate wet day frequency (a) climatology (shaded contours in pentads), (b) intensity-frequency map showing the percentage of the total number of seasons which consist of at least 20 wet days, and (c) trends (wet days decade⁻¹). Hatching denotes areas of significant trends calculated over the period 1981/1982–2018/2019. (d) Trends in GIMMS-NDVI-3g for February calculated over 1982–2015 with stippling denoting significant trends. DJF, December–February.

4. Moderate Wet Days

Figure 2a plots the mean number of moderate DJF wet days (10–30 mm/day). This criterion was chosen from what is optimal for intensive cropping (rather than damaging heavy rainfall >50 mm/day). Over the relatively wet summer rainfall region of eastern South Africa, important for maize, a moderate wet day occurs on about 10–16 days during the 90-days season on average.

Highest mean frequencies in moderate wet days are found over the southern Congo and northern and east coastal Madagascar (28–38 out of a maximum of 90 days) where northwesterly monsoonal and easterly trade winds impact, respectively, on significant topography. Southwestern Madagascar is a rain shadow and hence shows lower frequencies, although still comparable with those over most of southeastern Africa. The high frequencies over the southern Congo and northern Mozambique are near the low-level moisture convergence zones over land and the western Indian Ocean moisture source (Reason et al., 2006). Other topographic influences are evident on the Zimbabwe/Mozambique border, along the windward Drakensberg escarpment in eastern South Africa and downstream of Lake Malawi where the topography rises quickly from <300 to >1,200 m. Relatively high frequency occurs near the central Angolan highlands on the northern boundary of the Angola Low where there is often convergence between easterlies from the Indian Ocean and northwesterlies from the tropical South East Atlantic (Cook et al., 2004). For ON (unshown), high frequencies are confined to the northern Congo Basin and high topography of South Africa, Zimbabwe, and Madagascar.

The intensity-frequency map (Figure 2b) shows that over northern and central Madagascar and near the Zambia/DR Congo border, nearly all the 38 summers are made up of 20 or more moderate wet days (at least two every 9 days). This statistic reduces to about 75–90% of the seasons satisfying that criterion over the broader swath of wetter tropical convergence regions stretching from the northern Mozambique coast west to central Angola. The topographic influences of mountains in Madagascar, eastern Zimbabwe, central Mozambique, Malawi, and eastern South Africa are all evident although for the latter the statistic reduces to 25%–45% satisfying the criterion of at least 20 or more moderate wet days per season.

Large areas of statistically significant increasing trend in DJF moderate wet day frequency exist in central Angola, to the northwest of the typical Angola Low position, near the Zambian/DR Congo border, western Zimbabwe/eastern Botswana, and the northern tip of Madagascar (Figure 2c). In South Africa, two areas of significant increase are evident, one stretching northwest from the central Drakensberg toward Johannesburg and another stretching southwest from the border with Lesotho. Significant trends in rainfall totals (unshown) match up with all these areas as well as exist more broadly in Botswana and eastern South Africa. The two South African as well as the Angolan region of significant wet day trends are important existing agricultural areas whereas the others are sparsely settled. The magnitudes are about an extra 1–3 wet days per decade in-

crease on the climatology of about 7–12 such days per summer in western Zimbabwe/eastern Botswana, 12–15 such days in the central Drakensberg region, 20–28 days in central Angola, and about 28–35 near the Zambia/DR Congo border. A few areas of significant decreases occur in tropical southern Africa, notably in southern DR Congo which when viewed with the increase to its south suggests that the convergence zone here might have shifted slightly south during 1982–2019 and in coastal Tanzania. In general, the overall

patterns in Figure 2c are very similar to those for light (2–9 mm/day) trends (unshown) except in western/central Angola where there is a significant decreasing trend. For heavy wet days (>30 mm/day, unshown), there are significant increases (decreases) in eastern Zimbabwe, southern LRV and southeastern Mozambique (central and northwestern Madagascar, southwestern Tanzania). The increasing trend in moderate wet days in central South Africa combined with the broader region there of decreasing dry spell trend (Figure 1c) is further evidence of weakening of the strong diagonal gradient. Similarly, Figures 1d and 2c indicate that the drought corridor has weakened in the western LRV and eastern Botswana. Figure 2d shows a significant “greening” trend in February, particularly in the diagonal and meridional gradient regions consistent with the dry spell and wet day trends for DJF. Since NDVI in southern Africa typically responds 1–2 months after rainfall (Richard & Poccard, 1998), February was chosen.

For ON (unshown), there are significant decreasing trends in wet day frequency over parts of the diagonal gradient in South Africa, again consistent with early summer drying climate projections (Munday & Washington, 2019) and the December NDVI (unshown) indicates large areas of “browning.”

If daily satellite derived data (TRMM (0.25°) (Kummerow et al., 1998) or NOAA PERSIANN-CDR (0.25°) (Ashouri et al., 2015; Nguyen et al., 2019)) are used, very similar gradients and trends to Figures 1 and 2 result (unshown). Although there are some small differences in detail which necessarily result from the different resolution, processing algorithms, or shorter data records compared to CHIRPS, this consistency provides confidence in robustness of the results. However, the reduction in station coverage in some areas and changing satellite methodologies during the period means that caution needs to be taken. CHIRPS rainfall anomalies are highly correlated with station data over the Eastern Cape (Mahlalela et al., 2020) as are station-derived dry spells in the gradient region (Figure S2).

5. Potential Mechanisms

Potential mechanisms are investigated for two agriculturally important areas —Region 1 (diagonal gradient, southwest of Lesotho) and Region 2 (meridional gradient, part of the drought corridor extending from western Botswana to the central LRV).

Figure 3a indicates that DJF dry spells in Region 1 are associated with a stronger midlevel Botswana High and negative Southern Annular Mode (SAM)-like pattern with cyclonic anomaly south of South Africa. These patterns imply more subsidence/reduced cloud bands over South Africa and increased westerly advection of cool, dry Atlantic air over the southern landmass (Figures 3b and 3e, Figure S3a) consistent with literature for rainfall totals (Driver & Reason, 2017; Mulenga et al., 2003; Reason, 2016). The corresponding plots for moderate wet days are essentially the reverse (unshown) but with a larger area of significant correlation right across the tropics. The latter suggests ENSO relationships, indeed SST correlations show strong El Niño (La Niña) patterns in the dry spell (wet day) case for the Pacific and South Atlantic but less so for the Indian Ocean (Colberg et al., 2004; Reason et al., 2000) (Figure S3b). Figures 3c and 3d show significant correlations between the dry spell/wet day time series and those for ENSO, SAM, and Botswana High. Five year rolling correlations indicate coefficients >0.6 for ENSO/Botswana High except during 2003–2007 when they briefly change sign. SAM is more variable suggesting its relationship is less robust.

Figure 4a suggests that Region 2 DJF dry spells are linked with a weaker Mascarene High and stronger Mozambique Channel Trough (MCT) which acts to advect less moist marine Indian Ocean air toward the LRV with less penetration of this moisture into the mainland (Barimalala et al., 2018, 2020). Strong relative subsidence is apparent over the mainland implying less cloud bands/rainfall there and more over Madagascar (Hart et al., 2018) where there is also enhanced easterly moisture flux (Figures 4b and 4e and Figure S4a). Westerly moisture flux anomalies over southern Mozambique imply less moisture advection into Region 2 favoring dry spells. The patterns for moderate wet days (unshown) are essentially the reverse. SST correlations (Figure S4b) show weak ENSO Modoki patterns in the Pacific and a strong negative (positive) phase subtropical Indian Ocean dipole (SIOD) for dry spells (wet days) consistent with literature for rainfall totals (Behera & Yamagata, 2001; Reason, 2001, 2002). Figures 4c and 4d show significant correlations between the dry spell/wet day time series and the SIOD with rolling correlations strong except for 1999–2003, 2009–2010, and 2015.

For ON, there are significant correlations with ENSO for both Regions 1 and 2 but they are not as strong as in DJF, consistent with the phasing of ENSO impacts on southern African rainfall totals.

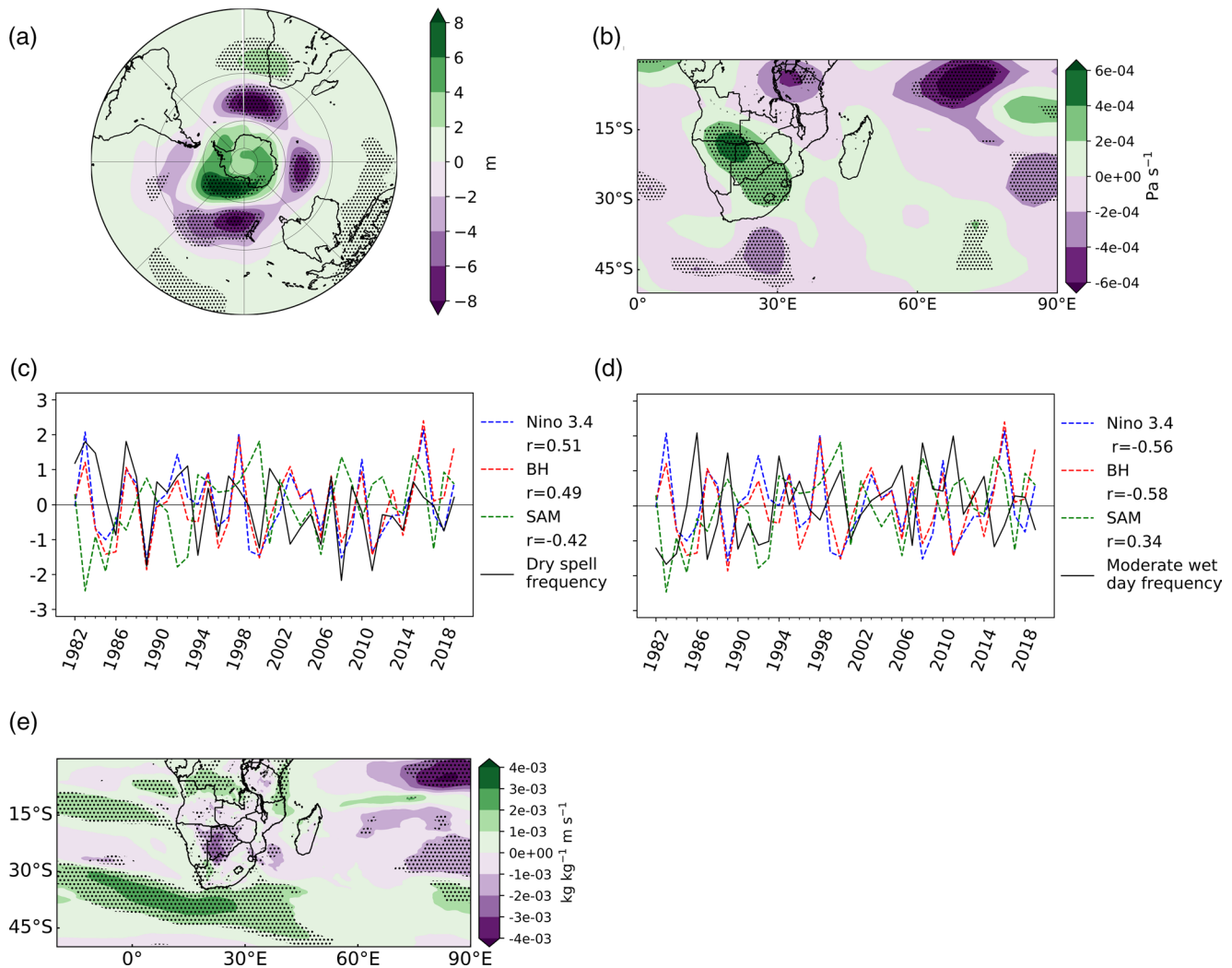


Figure 3. Regression between dry spell frequency over Region 1 and (a) 500 hPa geopotential height, (b) 500 hPa omega, (e) 850 hPa moisture flux. Stippling denotes significance at 95%. Panels (c) and (d) plot time series of DJF region one dry spell and moderate wet day frequency together with indices of ENSO (Niño 3.4), the Botswana High (as in Driver and Reason [2017]) and SAM (as in Marshall [1993]) and their corresponding correlation coefficients (all significant at 95%). DJF, December-February; SAM, Southern Annular Mode.

6. Conclusions

Understanding rainy season characteristics other than totals is more helpful to user groups. Here, two such characteristics (dry spell frequency and moderate wet day occurrence) are analyzed for December-February, the main rainy season for most of southern Africa and the crucial period for the staple crop of maize, to find that two strong gradients (diagonal and meridional) exist in dry spell frequency across the region. A similar diagonal gradient but northward shifted meridional gradient exists in the planting season (October-November).

A diagonal gradient extends from southwestern Angola southeastwards across the western Kalahari and Karoo deserts to the African south coast, roughly marking the westernmost location of cloud bands that bring most of the summer rainfall. Over South Africa, the eastern edge of this gradient indicates the transition from sheep farming to maize in the wetter areas to the east/northeast. The meridional gradient extends west from the Limpopo River Valley (LRV) across central Botswana and Namibia in DJF and along $\sim 14\text{--}16^\circ\text{S}$ in ON. These gradients are also areas where at least half of the rainy season is made up of dry spells during $>50\%$ of the 38 summers analyzed. Applying that criterion to 21 years of 2.5° CMAP data, Usman and Reason (2004) defined the $20\text{--}25^\circ\text{S}$ zone across southern Africa as the drought corridor based on its

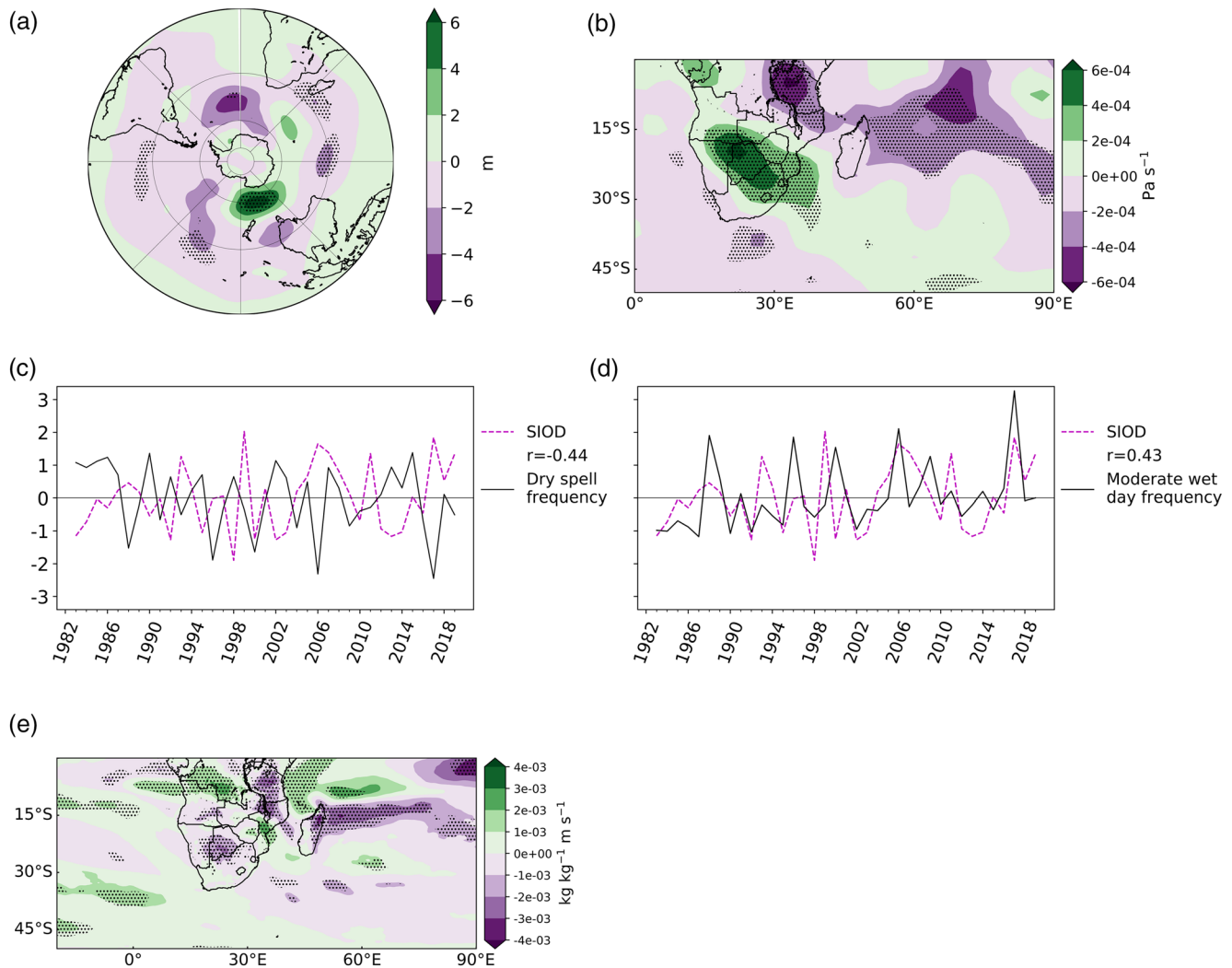


Figure 4. As for Figure 3 except for region two and time series show the South Indian Ocean subtropical dipole (as in Behera and Yamagata [2001]) and correlation coefficients (significant at 95%). ENSO, the Botswana High and SAM do not show significant correlations for region two and hence are not plotted. SAM, Southern Annular Mode.

susceptibility to drought during DJF. Based on 38 years high-resolution CHIRPS data, the drought corridor is much better defined, revealing a core along 22–23°S near the Zimbabwe/South Africa border for which 85–100% of the summers are dry more than half of the time. A spurious secondary maximum along the southern Mozambique coast in Usman and Reason (2004) no longer exists in the CHIRPS analysis. In ON, there is a second, previously unknown, drought corridor bordering the Zambezi River which has important implications for both agriculture and the crucial hydroelectric dams here which Zambia and Zimbabwe depend on. The trend analysis indicates a statistically significant decrease in DJF dry spells along much of the diagonal gradient during the period but increase in ON consistent with climate model projections of early summer drying in southern Africa (Munday & Washington, 2019). An area just south of the core of the meridional gradient also shows significant decreasing DJF trends as do the south coast of Mozambique and a large area in western Zimbabwe/northern Botswana. However, in summer 2018–2019, there were 1–3 standard deviation increases in dry spell frequencies (unshown) near the diagonal gradient in South Africa as well as over southern Zambia/northwestern Zimbabwe leading to ongoing power shortages due to massive drops in the hydroelectric dam of Lake Kariba and widespread famine.

Despite being located in the generally wetter eastern half of southern Africa and near major moisture sources of the western Indian Ocean, the core LRV of the drought corridor also stands out in the climatology map

of moderate wet days as a relative minimum. It is suggested that this is related to local topography and its position relative to the MCT that acts to divert moisture away from this part of southern Africa (Barimalala et al., 2018, 2020). Topographic influences on moderate wet day and dry spell frequencies are clearly apparent in the climatologies. The windward side of the mountains stand out as areas where at least 25% of DJF seasons contain >20 moderate wet days out of a possible 90 per season. Near the tropical convergence zones, 75–100% of these seasons satisfy that criterion. Statistically significant increasing trends in moderate wet days are found over central Angola, northern Zambia, a large northern Botswana/western Zimbabwe region, and some of the important agricultural areas of central South Africa.

Dry spell frequencies/wet days in the diagonal (meridional) gradient regions appear related to ENSO, SAM, Botswana High (SIOD) which cause changes in subsidence and convective cloud/cloud bands across southern Africa. Future work needs to investigate these mechanisms further to provide robust projections that can be used for planning and mitigation purposes.

Data Availability Statement

Publicly used data sets for this research are available from the following repositories:

- The CHIRPS rainfall data set was obtained from <https://data.chc.ucsb.edu/products/CHIRPS-2.0/>
- NCEP II data were obtained from <https://psl.noaa.gov/data/gridded/data.ncep.reanalysis2.pressure.html>
- PERSIANN data were obtained from <https://chrsdata.eng.uci.edu/>
- ERA5 data were obtained from <https://cds.climate.copernicus.eu/cdsapp#!/dataset/reanalysis-era5-pressure-levels-monthly-means?tab=form>
- GIMMS-NDVI-3g is available from <https://ecocast.arc.nasa.gov/data/pub/gimms/3g.v1/>
- Station rainfall data from the South African Weather Service are available for research purposes via a direct request to www.weathersa.co.za

Acknowledgments

ACCESS NRF and UCT Advancing Womxn Fellowship funding helped support the MSc research of WT and with data processing costs. We thank the South African Weather Service for providing daily rain-gauge data and two reviewers for helpful comments which improved the manuscript.

References

- Ashouri, H., Hsu, K.-L., Sorooshian, S., Braithwaite, D. K., Knapp, K. R., Cecil, L. D., et al. (2015). PERSIANN-CDR: Daily precipitation climate data record from multi-satellite observations for hydrological and climate studies. *Bulletin of the American Meteorological Society*, 96(1), 69–83. <https://doi.org/10.1175/BAMS-D-13-00068.1>
- Barimalala, R., Blamey, R. C., Desbiolles, F., & Reason, C. J. C. (2020). Variability in the Mozambique Channel Trough and impacts on southeast African rainfall. *Journal of Climate*, 33(2), 749–765. <https://doi.org/10.1175/JCLI-D-19-0267.1>
- Barimalala, R., Desbiolles, F., Blamey, R. C., & Reason, C. J. C. (2018). Madagascar influence on the South Indian Ocean convergence zone, the Mozambique Channel Trough and southern African rainfall. *Geophysical Research Letters*, 45, 11380–11389. <https://doi.org/10.1029/2018GL079964>
- Behera, S. K., & Yamagata, T. (2001). Subtropical SST dipole events in the southern Indian Ocean. *Geophysical Research Letters*, 28(2), 327–330. <https://doi.org/10.1029/2000GL011451>
- Blamey, R. C., Kolusu, S., Mahlalela, P., Todd, M., & Reason, C. J. C. (2018). The role of regional circulation features in regulating El Niño climate impacts over southern Africa: A comparison of the 2015/2016 drought with previous events. *International Journal of Climatology*, 38(11), 4276–4295. <https://doi.org/10.1002/joc.5668>
- Blamey, R. C., Middleton, C., Lennard, C., & Reason, C. J. C. (2017). A climatology of potential severe convective environments across South Africa. *Climate Dynamics*, 49(5–6), 2161–2178. <https://doi.org/10.1007/s00382-016-3434-7>
- Colberg, F., Reason, C., & Rodgers, K. (2004). South Atlantic response to El Niño–Southern Oscillation induced climate variability in an ocean general circulation model. *Journal of Geophysical Research*, 109, C12015. <https://doi.org/10.1029/2004JC002301>
- Cook, C., Reason, C. J. C., & Hewitson, B. C. (2004). Wet and dry spells within particularly wet and dry summers in the South African summer rainfall region. *Climate Research*, 26(1), 17–31. <https://doi.org/10.3354/cr026017>
- Driver, P., & Reason, C. J. C. (2017). Variability in the Botswana High and its relationships with rainfall and temperature characteristics over southern Africa. *International Journal of Climatology*, 37, 570–581. <https://doi.org/10.1002/joc.5022>
- Fauchereau, N., Pohl, B., Reason, C. J. C., Rouault, M., & Richard, Y. (2009). Recurrent daily OLR patterns in the southern Africa/southwest Indian Ocean region, implications for South African rainfall and teleconnections. *Climate Dynamics*, 32(4), 575–591. <https://doi.org/10.1007/s00382-008-0426-2>
- FEWS NET. (2020). *High food assistance needs persist due to consecutive droughts and erratic 2019/20 rainfall, Southern Africa Food Security Alert*. Retrieved from https://fews.net/sites/default/files/documents/reports/Southern%20Africa%20Alert_04022020_0.pdf
- Funk, C., Peterson, P., Landsfeld, M., Pedreros, D., Verdin, J., Shukla, S., et al. (2015). The climate hazards infrared precipitation with stations—A new environmental record for monitoring extremes. *Scientific Data*, 2(1), 150066. <https://doi.org/10.1038/sdata.2015.66>
- Hachigonta, S., & Reason, C. J. C. (2006). Interannual variability in dry and wet spell characteristics over Zambia. *Climate Research*, 32(1), 49–62. <https://doi.org/10.3354/cr032049>
- Hart, N. C. G., Reason, C. J. C., & Fauchereau, N. (2013). Cloud bands over southern Africa: Seasonality, contribution to rainfall variability and modulation by the MJO. *Climate Dynamics*, 41(5–6), 1199–1212. <https://doi.org/10.1007/s00382-012-1589-4>
- Hart, N. C. G., Washington, R., & Reason, C. J. C. (2018). On the likelihood of tropical–extratropical cloud bands in the south Indian convergence zone during ENSO events. *Journal of Climate*, 31(7), 2797–2817. <https://doi.org/10.1175/JCLI-D-17-0221.1>

- Kendall, M. G. (1975). *Rank correlation methods* (4th ed.). London: Charles Griffin.
- Kummerow, C., Barnes, W., Kozu, T., Shiue, J., & Simpson, J. (1998). The tropical rainfall measuring mission (TRMM) sensor package. *Journal of Atmospheric and Oceanic Technology*, 15(3), 809–817. [https://doi.org/10.1175/1520-0426\(1998\)015<0809:TRMMT>2.0.CO;2](https://doi.org/10.1175/1520-0426(1998)015<0809:TRMMT>2.0.CO;2)
- Landman, W. A., Sweijid, N., Masedi, N., & Minakawa, N. (2020). The development and prudent application of climate-based forecasts of seasonal malaria in the Limpopo province in South Africa. *Environmental Development*, 35, 100522. <https://doi.org/10.1016/j.envdev.2020.100522>
- Mahlalela, P., Blamey, R., Hart, N., & Reason, C. J. C. (2020). Drought in the Eastern Cape region of South Africa and trends in rainfall characteristics. *Climate Dynamics*, 55, 2743–2759. <https://doi.org/10.1007/s00382-020-05413-0>
- Malherbe, J., Engelbrecht, F. A., Landman, W. A., & Engelbrecht, C. J. (2012). Tropical systems from the southwest Indian Ocean making landfall over the Limpopo River Basin, southern Africa: A historical perspective. *International Journal of Climatology*, 32(7), 1018–1032. <https://doi.org/10.1002/joc.2320>
- Mann, H. B. (1945). Nonparametric tests against trend. *Econometrica*, 13(3), 245–259. <https://doi.org/10.2307/1907187>
- Mapande, A. T., & Reason, C. J. C. (2005). Links between rainfall variability on intraseasonal and interannual scales over western Tanzania and regional circulation and SST patterns. *Meteorology and Atmospheric Physics*, 89(1–4), 215–234. <https://doi.org/10.1007/s00703-005-0130-2>
- Mulenga, H., Rouault, M., & Reason, C. (2003). Dry summers over northeastern South Africa and associated circulation anomalies. *Climate Research*, 25(1), 29–41. <https://doi.org/10.3354/cr025029>
- Munday, C., & Washington, R. (2019). Controls on the diversity in climate model projections of early summer drying over southern Africa. *Journal of Climate*, 32, 3707–3725. <https://doi.org/10.1175/JCLI-D-18-0463.1>
- Munodawafa, A. (2012). The effect of rainfall characteristics and tillage on sheet erosion and maize grain yield in semiarid conditions and granitic sandy soils of Zimbabwe. *Applied and Environmental Soil Science*, 2012, 243815. <https://doi.org/10.1155/2012/243815>
- Nguyen, P., Shearer, E. J., Tran, H., Ombadi, M., Hayatbini, N., Palacios, T., et al. (2019). The CHRS Data Portal, an easily accessible public repository for PERSIANN global satellite precipitation data. *Scientific Data*, 6(1), 180296. <https://doi.org/10.1038/sdata.2018.296>
- Phillips, J., Cane, M. A., & Rosenzweig, C. (1998). ENSO, seasonal rainfall patterns and simulated maize yield variability in Zimbabwe. *Agricultural and Forest Meteorology*, 90(1–2), 39–50. [https://doi.org/10.1016/S0168-1923\(97\)00095-6](https://doi.org/10.1016/S0168-1923(97)00095-6)
- Pinzon, J., & Tucker, C. J. (2014). A non-stationary 1981–2012 AVHRR NDVI_{3g} time series. *Remote Sensing*, 6(8), 6929–6960. <https://doi.org/10.3390/rs6086929>
- Rapolaki, R. S., Blamey, R. C., Hermes, J. C., & Reason, C. J. C. (2019). A classification of synoptic weather patterns linked to extreme rainfall over the Limpopo River Basin in southern Africa. *Climate Dynamics*, 53(3–4), 2265–2279. <https://doi.org/10.1007/s00382-019-04829-7>
- Rapolaki, R. S., Blamey, R. C., Hermes, J. C., & Reason, C. J. C. (2020). Moisture sources associated with heavy rainfall over the Limpopo River Basin, southern Africa. *Climate Dynamics*, 55(5), 1473–1487. <https://doi.org/10.1007/s00382-020-05336-w>
- Reason, C. J. C. (2001). Subtropical Indian Ocean SST dipole events and southern African rainfall. *Geophysical Research Letters*, 28(11), 2225–2227. <https://doi.org/10.1029/2000GL012735>
- Reason, C. J. C. (2002). Sensitivity of the southern African circulation to dipole sea-surface temperature patterns in the south Indian Ocean. *International Journal of Climatology: A Journal of the Royal Meteorological Society*, 22(4), 377–393. <https://doi.org/10.1002/joc.744>
- Reason, C. J. C. (2016). The Bolivian, Botswana and Bilybara Highs and Southern Hemisphere drought/floods. *Geophysical Research Letters*, 43, 1280–1286. <https://doi.org/10.1002/2015GL067228>
- Reason, C. J. C., Allan, R. J., Lindesay, J. A., & Ansell, T. J. (2000). ENSO and climatic signals across the Indian Ocean basin in the global context: Part I, interannual composite patterns. *International Journal of Climatology: A Journal of the Royal Meteorological Society*, 20(11), 1285–1327. [https://doi.org/10.1002/1097-0088\(200009\)20:11<1285::AID-JOC536>3.0.CO;2-R](https://doi.org/10.1002/1097-0088(200009)20:11<1285::AID-JOC536>3.0.CO;2-R)
- Reason, C. J. C., Hachigonta, S., & Phaladi, R. F. (2005). Interannual variability in rainy season characteristics over the Limpopo region of southern Africa. *International Journal of Climatology*, 25(14), 1835–1853. <https://doi.org/10.1002/joc.1228>
- Reason, C. J. C., Landman, W., & Tennant, W. (2006). Seasonal to decadal prediction of southern African climate and its links with variability of the Atlantic Ocean. *Bulletin of the American Meteorological Society*, 87(7), 941–956. <https://doi.org/10.1175/BAMS-87-7-941>
- Richard, Y., & Pocard, I. (1998). A statistical study of NDVI sensitivity to seasonal and interannual rainfall variations in Southern Africa. *International Journal of Remote Sensing*, 19(15), 2907–2920. <https://doi.org/10.1080/01431169814343>
- Sen, P. K. (1968). Estimates of the regression coefficient based on Kendall's tau. *Journal of the American Statistical Association*, 63(324), 1379–1389. <https://doi.org/10.1080/01621459.1968.10480934>
- Tadross, M., Suarez, P., Lotsch, A., Hachigonta, S., Mdoka, M., Unganai, L., et al. (2007). Changes in growing-season rainfall characteristics and downscaled scenarios of change over southern Africa: Implications for growing maize. In *IPCC regional expert meeting on regional impacts, adaptation, vulnerability, and mitigation* (pp. 193–204). Fiji: Nadi.
- Tadross, M., Suarez, P., Lotsch, A., Hachigonta, S., Mdoka, M., Unganai, L., et al. (2009). Growing-season rainfall and scenarios of future change in southeast Africa: Implications for cultivating maize. *Climate Research*, 40(2–3), 147–161. <https://doi.org/10.3354/cr00821>
- Theil, H. (1950). A rank-invariant method of linear and polynomial regression analysis. *Proceedings of the Royal Netherlands Academy of Sciences*, 53(Part I), 386–392, Part II, 521–525, Part III, 1397–1412.
- Tyson, P. D. (1986). *Climatic change and variability in southern Africa*. Oxford: Oxford University Press.
- Usman, M. T., & Reason, C. J. C. (2004). Dry spell frequencies and their variability over southern Africa. *Climate Research*, 26(3), 199–211. <https://doi.org/10.3354/cr026199>